vised; however, Slater's assumption regarding the ordering of the hydrogens appears to be reasonable. In the first place, the expansion of the hydrogen bond in the transition supports such a view. In addition, if one assumes that the hydrogens 'belong' to the O_1 set of oxygens, and have been 'lost' by the O_2 set, then the observed lengthening of P, O_1 and contraction of P, O_2 could be a reasonable consequence. Furthermore, the change in the ionic environment of the K's would act so as to displace them in the proper direction. This is evident from Fig. 8, in which the neighborhood of the K's is shown schematically.

The question remains as to how these changes could be 'triggered' in the transition. The hydrogen role has been emphasized heretofore, but a more complete answer might be the following. As the crystal is cooled, the hydrogen bonds begin to contract in the X, Y plane. The effect of this is to destroy the equidistance of the KO_8 arrangement. This causes the K to build up a preferred vibration parallel to c, which in turn induces a similar preferred vibration in the PO_4 groups. Finally a critical temperature is reached, the Curie point, at which the K's 'lock in' to a position displaced from their previous centers of oscillation. The displaced K's then exert a polarizing influence on the PO_4 groups and an electrostatic influence on the hydrogens. In this way the P's become displaced within their O_4 tetrahedra and the hydrogens become more ordered.

The tentative model just described, or other such models that seem to fit the structural results reported here, will depend on future verification of the structural role of the hydrogens in the transition. The best approach to this seems to be through neutron diffraction. The results of the present investigation will greatly simplify such work, and should facilitate more extensive theoretical treatment of the general problem of the KH_2PO_4-type ferroelectrics as well.

References

Busch, G. & Scherrer, P. (1935). *Naturwissenschaften*, **23**, 737.

Cochran, W. (1951). *Acta Cryst.* **4**, 81.

Decker, H. C. J. de (1941). *Rev. Trav. chim. Pays-Bas*, **60**, 414.

Decker, H. C. J. de & MacGillavry, C. H. (1941). *Rec. Trav. chim. Pays-Bas*, **60**, 153.

Frazer, B. C. & Pepinsky, R. (1950). *Phys. Rev.* **80**, 124.

Internationale Tabellen zur Bestimmung von Kristallstrukturen (1944), revised ed. Ann Arbor: Edwards.

Pepinsky, R. (1947). *J. Appl. Phys.* **18**, 601.

Quervain, M. de (1944). *Helv. phys. Acta*, **17**, 509.

Slater, J. C. (1941). *J. Chem. Phys.* **9**, 16.

Ubbelohde, A. R. & Woodward, I. (1947). *Proc. Roy. Soc.* A, **188**, 358.

Viervoll, H. & Ögrim, O. (1949). *Acta Cryst.* **2**, 277.

West, J. (1930). *Z. Krystallogr.* **74**, 306.

Yomosa, S. & Nagamiya, T. (1949). *Prog. Theor. Phys.* **4**, 263.

Acta Cryst. (1953). **6**, 285

The Structure of $MnAl_6$

By A. D. I. Nicol

Crystallographic Laboratory, Cavendish Laboratory, Cambridge, England and B.S.A. Group Research Centre, Sheffield, England

(*Received* 21 *October* 1952)

The structure of the compound $MnAl_6$ has been determined. A brief description is given of the experimental methods used, together with an estimate of the accuracy obtained in the structure analysis. Electron counts and Brillouin zone measurements provide qualitative evidence in support of Raynor's theory that in electron-rich phases the transitional metal atoms absorb electrons. Some interesting Mn–Al and Al–Al interatomic distances are discussed in detail and it is suggested that they, too, provide indirect evidence of the importance of electronic factors in the formation of this structure.

1. Introduction

The determination of the structure of $MnAl_6$ forms part of a programme of structural work on the aluminium-rich phases occurring in binary and ternary alloys of aluminium with the transitional metals of the first long period. The work of Raynor and his collaborators in Birmingham (see, for example, Raynor & Wakeman, 1947; Raynor & Waldron, 1948; Pratt & Raynor, 1951) has indicated that the investigation of these alloys is likely to be important for the further theoretical study of alloy formation. The present research was undertaken with the intention of helping to establish some of the factors which govern the formation of these stable intermetallic compounds.

Assuming that these phases may be regarded as electron compounds, interesting relationships have been shown to exist between them. Raynor suggests that the role of the transitional metal atoms is to prevent the aluminium atoms from contributing their full number of valency electrons to the structure as free electrons; it is supposed that some of these electrons are absorbed into the vacancies which exist in the atomic orbitals of the 3*d* shell (Pauling 1938, 1949). A direct method of observing such an effect is to count the numbers of electrons associated with the atomic peaks obtained from an accurate structure determination. Evidence of this type, which appears to support the theory, has already been provided by Douglas (1950) for cobalt in Co_2Al_9 and Robinson (1952) for manganese atoms in Mn_3SiAl_9.

The existence of the compound $MnAl_6$ was first noted by Köster & Bechthold (1938) and has been confirmed by several investigators (Phillips, 1943; Raynor & Hume-Rothery, 1943). Using single crystals, Hofmann (1938) found an orthorhombic unit cell for the compound, with dimensions in good agreement with those obtained by the author. I am indebted to Prof. Raynor and Dr Wakeman for the specimens used during the present investigation.

2. Specimens

The powder pattern of $MnAl_6$ is too complex to interpret without ambiguity and it was therefore necessary to use single crystals. According to Raynor & Wakeman (1947) these crystals, which were electrolytically extracted from an aluminium–manganese–zinc alloy, might contain a small amount of zinc impurity. A chemical analysis of the crystals gave a formula $Zn_{0\cdot03}Mn_{0\cdot96}Al_6$ which indicates the possibility that zinc replaces the manganese atom for atom. This amount of impurity, however, is too small to have any significant effect on the structure determination. The crystals were prismatic needles of a silver-grey colour, with very well formed and highly reflecting side faces. The needle cross-sections were rhombic with an average angle of 81·6°. They were brittle but by cutting across the needle axis specimens were prepared which approximated to a cube of side 0·015 cm.

3. Experimental technique

Only a brief outline of the methods used in the determination of the structure, together with a discussion of its main features, will be given in this paper. Full details are available elsewhere (Nicol, 1951).

The methods of collecting the intensity data were influenced by two considerations. The first aim of the research was to obtain the atomic parameters with the greatest accuracy possible within the limitations imposed by two-dimensional Fourier methods. This entailed the inclusion of all reflexions observable with the shortest radiation available, namely Mo $K\alpha$ radiation. Secondly, it has been calculated that only reflexions with $\sin\theta/\lambda$ less than 0·6 Å^{-1} are sensitive to changes of electron distribution in the 3*d* shell of manganese. These reflexions, therefore, should be measured with great accuracy. Ideally the intensities should be measured on an absolute scale. Attempts were made to do this by photographic methods involving the use of monochromatic $K\alpha_1$ radiation and an aluminium specimen as a standard. The exposure times were large and the limited number of photographs obtained were found for various purely practical reasons to be unsuitable for very accurate photometry.

(i) *Photographic methods used in the collection of intensity data*

Oscillation photographs using a multiple-film technique were taken, the higher orders being recorded in a camera modified to take back-reflexion photographs (Farquhar & Lipson, 1946). Mo $K\alpha$ radiation was used, for which the limiting value of $\sin\theta/\lambda$ is 1·41 Å^{-1}, and reflexions were recorded up to 1·403 Å^{-1}. The use of this radiation and of a small specimen of nearly cubic shape greatly reduced the effects of absorption. The intensities were estimated visually against a standard intensity scale prepared with the same crystal. An approximate correction for the increasing resolution of the $K\alpha$ doublet with increasing Bragg angle was made and the usual corrections for Lorentz and polarization factors were applied. For the final refinement of the structure both these corrected intensities I'_{hkl} and those measured on the counter spectrometer were reduced to an absolute scale in the usual way by means of a scaling factor (Cochran, 1951).

(ii) *Counter methods used in the collection of intensity data*

The needle axis of the crystals was parallel to the *c* dimension of the unit cell. The crystals were therefore of an ideal form for the measurement of the integrated intensity of the (*hk*0) reflexions as the regular cross-section enabled the absorption to be accurately calculated using the method suggested by Albrecht (1939). The specimen used in these experiments was 0·0712 cm. long, the side of the rhombic cross-section being 0·0215 cm. Cochran (1950) has described the spectrometer, to which only minor modifications were made for these measurements. Molybdenum radiation was again used and the Geiger counter was krypton filled with an alcohol quencher. Two sets of intensity measurements were made, one using a lithium fluoride monochromatizing crystal which reduced the background radiation and enabled the important strong low-angle reflexions to be measured with considerable accuracy, the second set using balanced Zn and SrO filters which ensured that a statistically significant count could be obtained for the weaker reflexions in a reasonable time. The two sets of readings were correlated. Using the second method, reflexions were measured up to $\sin\theta/\lambda = 1{\cdot}22$ Å^{-1}. In both sets the crystal was oscillated through an angle of 1–1½° and precautions were taken to ensure that effects due to harmonic radiations were eliminated. An idea of the balance obtained between the filters is given by the traces shown in Fig. 1.

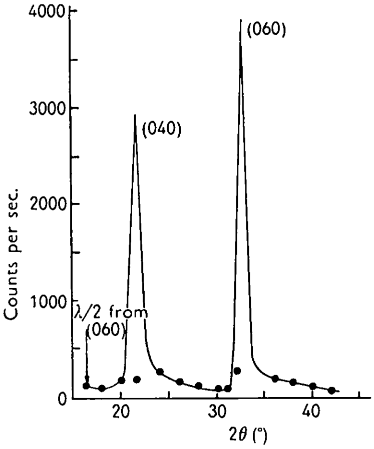

Fig. 1. Curves obtained to test the accuracy of the balanced filters. The full line curve was obtained with a Zr filter in the incident beam; Points indicate the readings obtained with a SrO filter in the beam. The crystal was stationary during each reading and was set at successive 2° intervals through the (040) and (060) reflecting positions.

Before correcting the integrated intensities for Lorentz, polarization and absorption effects, the counter readings were corrected for counter drift, cosmic background and X-ray background. Lost counts never amounted to more than 3% of the total number of counts recorded. In addition, in the case of the balanced filter readings a correction was made for the variable dispersion of the white radiation, lying between the K absorption edges of the filters, which passed through the counter slits.

The counter characteristics were not as good as could have been desired and it is felt that greater accuracy is possible using these methods. The agreement between the two sets of readings may be judged by the value of 0·055 obtained for the factor $(\sqrt{I'_M}-\sqrt{I'_B})\div\sqrt{I'_M}$ for the 30 strongest reflexions, where I'_M and I'_B are the corrected intensities using the monochromator and balanced filters respectively.

4. X-ray data

(i) *Unit cell and cell contents*

The unit cell dimensions were determined by a modification of the extrapolation method due to Farquhar & Lipson (1946). An orthorhombic cell was found with dimensions

$$a = 6{\cdot}4978 \pm 0{\cdot}0005,\ b = 7{\cdot}5518 \pm 0{\cdot}0005,$$
$$c = 8{\cdot}8703 \pm 0{\cdot}0005\ \text{Å},$$

which are in good agreement with Hofmann's values of $a = 6{\cdot}51$, $b = 7{\cdot}57$ and $c = 8{\cdot}87$ Å. The density determined by displacement was found to be $3{\cdot}27 \pm 0{\cdot}01$ g.cm.$^{-3}$, as compared with Hofmann's value of 3·09 g.cm.$^{-3}$, whilst that calculated on the basis of 4 manganese atoms and 24 aluminium atoms per unit cell is 3·3065 g.cm.$^{-3}$. The space group and final structure analysis support this choice of 4 units of $MnAl_6$ per unit cell. The small difference between the experimentally determined density and that calculated on this assumption could well be accounted for by the presence of minute air bubbles which could not be removed from the crystals.

(ii) *Space group*

The systematic absences are consistent with any one of the three space groups D_{2h}^{17}–$Ccmm$, C_{2v}^{12}–Ccm and C_{2v}^{16}–$Cc2m$, and the choice of the correct space group cannot be made on the basis of the cell contents which can be accommodated by all three. By analysing the intensity distribution according to the method described by Howells, Phillips & Rogers (1950) it was possible, however, to distinguish between the three. Wilson (1949) has shown that the probability distributions of the intensities are different in the case of centrosymmetric and non-centrosymmetric arrays. Of the three space groups only *Ccmm* is centrosymmetric, whilst *Ccm* has a centre of symmetry only in the (*hk*0)

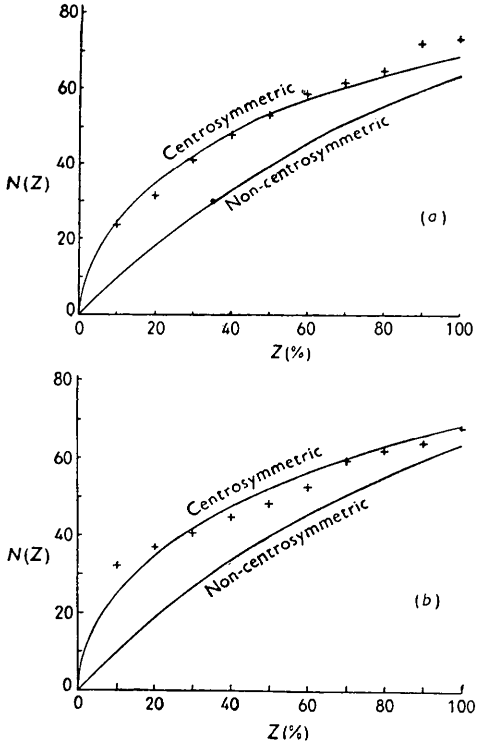

Fig. 2. (*a*) Intensity distribution for (*hk*0) reflexions. (*b*) Intensity distribution for (*h*0*l*) reflexions. The full lines give the theoretical distributions. $N(Z)$ is the number of reflexions with an intensity less than or equal to Z% of the local average intensity.

projection and *Cc2m* in the (*h0l*) projection. The results of the analysis (Fig. 2) clearly indicate a centrosymmetrical array, and the holohedral space group *Ccmm* was finally assigned to the compound. That in fact a correct choice was made is shown by the good agreement obtained between the observed and calculated structure amplitudes after the final refinement of the structure (see § 5(ii)).

5. Determination of the structure

(i) *Procedure*

Patterson projections were prepared from the corrected (*hk*0) and (*h0l*) intensities. By combining the information provided by each, a set of co-ordinates was finally found for the 28 atoms which not only satisfied the positions of all the peaks in both projections but also accounted very well for their relative heights. The final selection was

4 Mn in 4(c): $x, 0, \frac{1}{4}$ with $x = 0{\cdot}457$;
8 Al_1 in 8(e): $0, y, 0$ with $y = 0{\cdot}327$;
8 Al_2 in 8(g): $x, 0, z$ with $x = 0{\cdot}140$ and $y = 0{\cdot}100$;
8 Al_3 in 8(f): $x, y, \frac{1}{4}$ with $x = 0{\cdot}290$ and $y = 0{\cdot}320$.

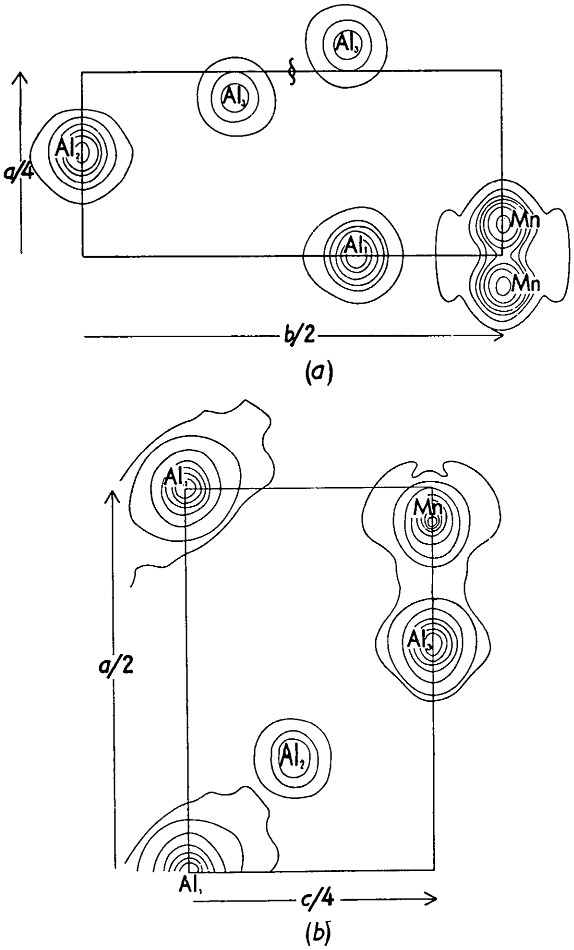

Fig. 3. (*a*) The asymmetric unit of the final (*hk*0) electron-density projection. (*b*) The asymmetric unit of the final (*h0l*) electron-density projection. No artificial convergence factor has been applied to either projection. The contours are drawn at intervals of 100 arbitrary units.

Both the (*hk*0) and (*h0l*) projections were refined by Fourier methods, using the counter data for the (*hk*0) projection and the photographic data for the (*h0l*) projection. The final projections without the use of any artificial convergence factor are shown in Fig. 3.

(ii) *Accuracy of atomic co-ordinates*

The final atomic co-ordinates given by the two projections are shown in Table 1. In column 3 the values of the parameters are given after correction for series termination by the F_c-synthesis method of Booth (1946). It will be seen that with the exception of the manganese peaks in the (*hk*0) projection there is little overlapping of peaks, and after allowance has been made for series-termination effects the remaining errors in the atomic co-ordinates are most probably due to experimental errors in the observed structure factors. Cruickshank (1949) has suggested a method of estimating these errors which depends on the determination of $\Delta F = F_o - F_c$. The probable errors are shown in column 4 of Table 1. It should be noted that the agreement in the x co-ordinates derived from the two projections is good and that the differences $x_{\mathrm{Mn}} = 0{\cdot}0006$, $x_{\mathrm{Al}_2} = 0{\cdot}0005$ and $x_{\mathrm{Al}_3} = 0{\cdot}0018$ are less than the experimental probable errors. When this occurs it is likely that the random errors have been overestimated. Additional confirmation of the accuracy of the atomic co-ordinates is supplied by the $F_o - F_c$ projections described in § 7(ii). The atomic co-ordinates finally selected, together with their standard deviations, are given in Table 2.

Table 1. *Atomic parameters*

(*a*) From (*hk*0) projection

		1	2	3	4
x	Mn	0·4571	0·0002	0·4573	0·0014
y	Al_1	0·3256	−0·0016	0·3240	0·0024
x	Al_2	0·1401	0·0006	0·1407	0·0021
x	Al_3	0·2847	−0·0027	0·2820	0·0034
y		0·3172	−0·0002	0·3170	0·0020

(*b*) From (*h0l*) projection

		1	2	3	4
x	Mn	0·4568	−0·0001	0·4567	0·0012
x	Al_2	0·1401	0·0001	0·1402	0·0011
z		0·1012	0·0008	0·1020	0·0020
x	Al_3	0·2854	−0·0016	0·2838	0·0016

1. Parameter obtained from projection.
2. Difference between 1 and parameter obtained from F_c synthesis.
3. Parameter corrected for series-termination errors.
4. Probable error in parameter.

The reliability of the proposed structure may also be judged by the values obtained for the arbitrary factor $R = \Sigma|F_o - F_c| \div \Sigma|F_o|$ which for the final (*h0l*) synthesis is 0·15. The value for the final (*hk*0) synthesis is 0·19, but if allowance is made for extinction effects

Table 2. *Atomic parameters finally selected and their standard deviations*

	x	$\sigma(x)$	y	$\sigma(y)$	z	$\sigma(z)$
Mn	0·4567	0·0018	0	—	$\frac{1}{4}$	—
Al_1	0	—	0·3240	0·0035	0	—
Al_2	0·1402	0·0016	0	—	0·1020	0·0029
Al_3	0·2838	0·0022	0·3170	0·0029	$\frac{1}{4}$	—

in the four strongest low-angle reflexions this value drops to 0·14. Strong support for the correctness of this structure, based on the holohedral space group, is given by the low R value of 0·11 for over 130 general (hkl) structure factors.

6. Description of the structure and discussion of interatomic distances

A prominent feature of both the Co_2Al_9 and Mn_3SiAl_9 structures is the layering of atoms parallel to a plane with low indices. It has been suggested by Robinson (1952) that this may be a characteristic feature of these compounds. The layering of atoms in the $MnAl_6$ structure is not so pronounced, but Fig. 4 shows that there are closely-packed, slightly puckered layers of aluminium atoms parallel to the (101) planes. Other layers can be distinguished parallel to (110) planes, but they are not so well-defined. It is interesting in this connection to note that the most characteristic feature of the crystals was the highly perfect development of the (110) faces.

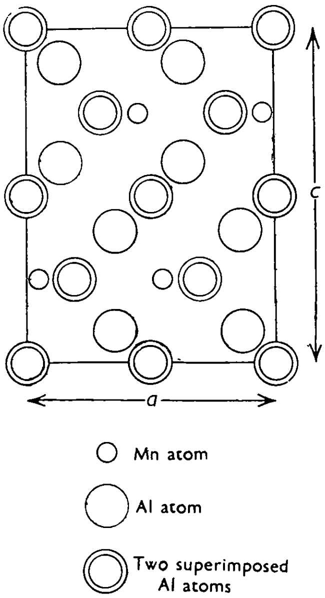

Fig. 4. Projection of $MnAl_6$ structure down b axis.

Fig. 5 shows the distribution of the atoms in the unit cell. The manganese atoms lie in sheets parallel to the (001) face at heights $\frac{1}{4}c$ and $\frac{3}{4}c$. One set of 8 aluminium atoms (Al_3) also lie in the (001) mirror planes at $\frac{1}{4}c$ and $\frac{3}{4}c$, each one having as nearest neighbours two manganese atoms in the same plane. Another set of 8 atoms (Al_1) lie in the c glide planes and are also shared between two manganese atoms, one in each of the (001) mirror planes. The remaining 8 aluminium atoms (Al_2) lie on the (010) mirror planes.

Each Al_2 atom has *one* manganese atom lying in the same plane, as nearest neighbour. The unit of the structure consists, therefore, of a manganese atom lying inside a complicated polyhedron formed by the 10 nearest aluminium atoms, 8 of which are shared between neighbouring polyhedra.

Details of the interatomic distances, together with their probable errors, are given in Table 3. The most interesting features are the small interatomic distance between the manganese atom and the unshared Al_2 atoms, and the very short Al_2–Al_2 distances. The Mn–Al_2 distance is considerably shorter than the value of 2·68 Å which would be deduced from the interatomic distances in the pure metals after allowance has been made for co-ordination number. The two Al_3 atoms at 2·54 Å are also significantly closer to the Mn atom. This division of the atoms surrounding the manganese atom into close and more distant neighbours bears a marked resemblance to the arrangement in Mn_3SiAl_9. In this structure the manganese atom is surrounded by two silicon and eight aluminium atoms, two of the aluminium atoms and the two silicon atoms lying significantly closer than the rest. Robinson (1952) has noted a similar division of the atoms surrounding the chromium atom in $Cr_4Si_4Al_{13}$, whilst in Co_2Al_9 (Douglas, 1950) one of the nine aluminium atoms surrounding the cobalt is also significantly closer.

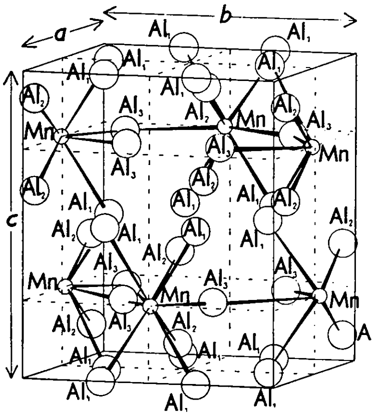

Fig. 5. Distribution of atoms in the unit cell of $MnAl_6$. The bonds between the manganese atoms and their aluminium neighbours are shown.

An upper limit of 2·9 Å was taken for the distance between aluminium atoms which are to be considered

Table 3. *Interatomic distances in* $MnAl_6$

Atom	Neighbour	No. of neighbours	Distance (Å)	Probable error (Å)
Mn	Al_1	4	2·60	0·025
	Al_2	2	2·435	0·025
	Al_3	2	2·64	0·03
	Al_3	2	2·54	0·03
Al_1	Mn	2	2·60	0·025
	Al_1	1	2·64	0·035
	Al_2	2	2·76	0·04
	Al_2	2	2·84	0·04
	Al_3	2	2·84	0·03
	Al_3	2	2·88	0·03
Al_2	Mn	1	2·435	0·025
	Al_1	2	2·76	0·04
	Al_1	2	2·84	0·04
	Al_2	1	2·57	0·03
	Al_2	1	2·62	0·03
	Al_3	2	2·89	0·045
	Al_3	2	2·77	0·045
Al_3	Mn	1	2·64	0·03
	Mn	1	2·54	0·03
	Al_1	2	2·84	0·03
	Al_1	2	2·88	0·03
	Al_2	2	2·89	0·045
	Al_2	2	2·77	0·045
	Al_3	1	2·77	0·04

Average Mn–Al distance = 2·56 Å with standard deviation 0·04 Å.

Average Al–Al distance = 2·78 Å with standard deviation 0·057 Å.

as 'in contact', and the mean value of 2·78 Å with a standard deviation of 0·057 Å is in good agreement with the value of 2·79$_5$ Å found for the Mn_3SiAl_9 structure. The average interatomic distance in aluminium metal is 2·86 Å, but Axon & Hume-Rothery (1948) have shown that when allowance has been made for the overlap in the first Brillouin zone the best value of the atomic diameter is 2·71 Å. The distance between the Al_2 atoms is, however, much shorter than this or any previously reported distance, and it is worth examining in greater detail the evidence for the reality of these abnormally short distances.

The two Al_2 atoms with interatomic distances 2·57 Å lie in the same mirror plane and are related by a two-fold axis, and the co-ordinates of these two atoms can be written as $(\frac{1}{2}+x, \frac{1}{2}, \frac{1}{2}-z)$ and $(\frac{1}{2}-x, \frac{1}{2}, \frac{1}{2}+z)$ with appropriate values for the parameters x and z. The other two Al_2 atoms at a distance 2·62 Å also lie in the mirror plane and are related by the (001) mirror planes, their co-ordinates being of the form $(\frac{1}{2}+x, \frac{1}{2}, z)$ and $(\frac{1}{2}+x, \frac{1}{2}, \frac{1}{2}-z)$ with the same values of x and z. An error in the determination of the x parameter will have no effect upon the interatomic distance between these last two atoms, the only method of increasing the distance being to decrease the value of the z parameter. If this is done, however, the distance between the other pair of atoms will become shorter still, assuming no change in the x co-ordinate. The distance between the atoms with co-ordinates $(\frac{1}{2}+x, \frac{1}{2}, \frac{1}{2}-z)$ and $(\frac{1}{2}-x, \frac{1}{2}, \frac{1}{2}+z)$ can only be modified to a limited extent by increasing the value of the x parameter, as the already short interatomic distance between Mn and Al_2 of 2·43 Å will be still further reduced by any such change. Provided the correct space group has been chosen so that the Al_2 atoms are free to move only in the (010) mirror planes, these interatomic distances must be significantly short, and it is unlikely that a more accurate determination of the atomic parameters will produce an Al_2–Al_2 distance that varies much from 2·6 Å. The possible significance of these short bonds is discussed in § 7(i).

7. Evidence of electron transfer

(i) *Electron counts*

Counts of the total numbers of electrons associated with equal areas surrounding each peak in both the ($hk0$) and ($h0l$) electron-density projections are given in Table 4. The fact that the total number of electrons in the unit cell, 412, is not found in either projection means that the actual numbers given are not quantitatively correct. It is, however, highly suggestive that in both cases the number of electrons associated with the manganese peaks is in excess of the normal 25 for a neutral manganese atom, whilst the aluminium peaks are deficient in electrons, those for Al_2 giving the lowest counts of all. It is fortunate that in the ($h0l$) projection there are peaks corresponding to two superposed aluminium atoms, as well as to single aluminium and single manganese atoms, for this permits a comparison of the manganese peak with one of approximately the same magnitude, thus minimizing any errors due to wrong scaling. It is at once apparent that in every case the ratio of manganese count to aluminium count is higher than the 25:13 ratio to be expected if no absorption of electrons took place. In view of the short Mn–Al_2 distances, it seems reasonable to suggest that the aluminium atoms Al_2 may be considered as the donors of electrons to the manganese atoms. If this is so, it is possible to offer an explanation of the short Al_2–Al_2 distances.

Table 4. *Number of electrons associated with the atomic peaks*

Atom	($hk0$) projection	($h0l$) projection
2 Mn	54·3	—
Mn	—	27·9
2 Al_1	22·2	23·2
2 Al_2	21·4	—
Al_2	—	11·6
Al_3	11·8	—
2 Al_3	—	24·5
Background	29	11·3
Total	407	413·5

The total number of electrons in the unit cell is 412.

(ii) $F_o - F_c$ *syntheses*

A difference series is independent of the number of terms used in its evaluation and is therefore particularly suited to this problem of detecting any abnormal electron distribution in the manganese $3d$ shell as only the low-angle terms sensitive to a change in the distribution of the outer electrons need be used. Diffraction effects shown by this type of series are due to (a) wrong choice of atomic parameters, (b) incorrect temperature factors and (c) discrepancies between the atomic scattering factor parameters assumed in calculating F_c and those actually operative in determining F_o.

In both ($hk0$) and ($h0l$) projections only terms with $\sin\theta/\lambda < 0{\cdot}6$ Å^{-1} were included in the series. F_c was calculated from the expression

$$F_c = \mathcal{F}_c \exp\left[(-B\sin^2\theta/\lambda^2)\times 10^{-16}\right],$$

where $\mathcal{F}_c$ denotes the structure factor calculated for an atom at rest. The atomic scattering factors used are those given by Viervoll & Ögrim (1949) for neutral manganese and aluminium atoms. Various values of the temperature factor B, ranging from 0·5 to 0·8, were tried and, though changes in the diffraction effects occurred, the general appearance of the projections was similar to those shown in Fig. 6. In every case the most prominent feature was the excess of electron density around the position of the manganese peak. It is doubtful whether the experimental accuracy justifies further refinement and the electron counts given in Table 5 may be considered as corroborating the information derived from direct electron counts and discussed in § 7(i).

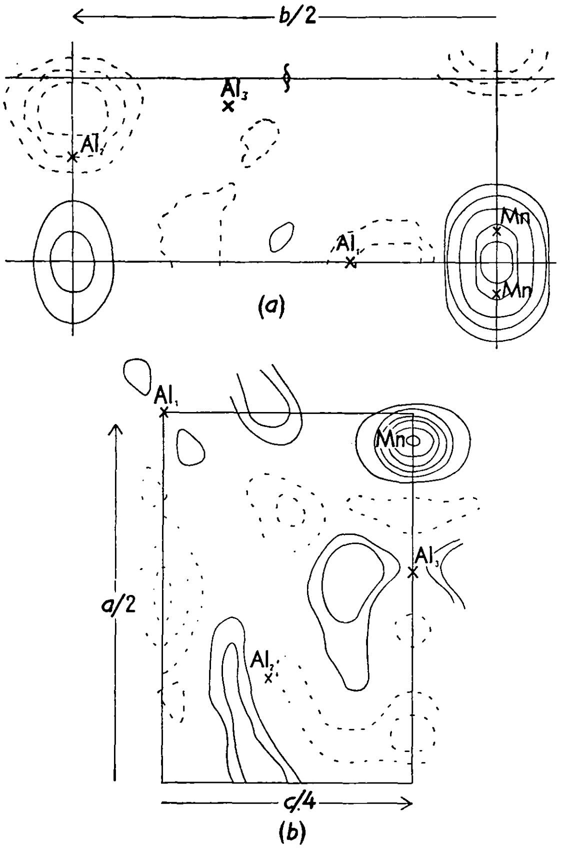

Fig. 6. (a) The asymmetric unit of the ($F_o - F_c$) projection for the ($hk0$) reflexions. Temperature factor $B = 0{\cdot}8\times 10^{-16}$ cm.^{2}. (b) The asymmetric unit of the ($F_o - F_c$) projection for the ($h0l$) reflexions. Temperature factor $B = 0{\cdot}5\times 10^{-16}$ cm.^{2}. The shift indicated for the Al$_2$ atom in both projections is less than the probable error given for the atomic coordinates.

Table 5. *Number of excess electrons associated with equal areas around the atomic positions in the* ($F_o - F_c$) *projections*

Atom	($hk0$) projection	($h0l$) projection
2 Mn	+2·4	—
Mn	—	+1·9
2 Al$_1$	−0·9	−0·7
2 Al$_2$	−1·3	—
Al$_2$	—	−0·9
Al$_3$	−0·2	—
2 Al$_3$	—	−0·3

The evidence for the presence of extra electrons in the manganese atom is thus very strong, and though too much weight should not be given to the numerical values obtained for the excess electron content it seems that it is about 2 electrons per manganese atom—certainly much less than the 3·66 electrons per atom of Raynor's hypothesis. The number given by Douglas for extra electrons in the cobalt peak of Co$_2$Al$_9$ is 1·7.

(iii) *First Brillouin zone*

The observation of a prominent Brillouin zone in these intermetallic compounds provides another method by which the role of the transitional metal atoms in their formation can be examined. If the theory of Jones (1934) for simple structures can be extended to cover these complicated ones, then the volume V of the Fermi distribution within the first zone can be used to calculate the average number of free electrons per atom, $2Vv$, for the structure, where v is the mean atomic volume. The zone is bounded by the first planes across which there is a large energy discontinuity. These planes correspond to a set of intense X-ray reflexions occurring, for a symmetrical zone, within a small range of $\sin\theta$. Such a group is observed on powder photographs of MnAl$_6$, and the planes are listed together with their F^2 values and their distances from the origin in k space in Table 6.

The dimensions of the zone lead to an electron : atom ratio lying between 1·35 corresponding to the volume of the inscribed sphere touching the (131) planes, and 1·96 for that touching the (114) planes. Assuming trivalent aluminium atoms and a negative valency of 3·66 for manganese, the calculated value of the ratio is 2·05, and it increases to 2·57 if zero valency is assumed for manganese. The Brillouin zone measure-

Table 6. *Planes contributing to the first Brillouin zone of* $MnAl_6$

$(h\,k\,l)$	Multiplicity	$\sin\theta/\lambda$ (Å^{-1})	$F^2\times10^{-2}$
1 3 1	8	0·2203	132
0 0 4	2	0·2255	216
2 0 3	4	0·2286	164
2 2 2	8	0·2322	166
3 1 0	4	0·2402	228
1 3 2	8	0·2411	237
3 1 1	8	0·2467	77
1 1 4	8	0·2473	137

ments therefore support the contention that the manganese atoms do in fact prevent the aluminium atoms from supplying their full three valency electrons to the structure.

(iv) *Interpretation of interatomic distances in terms of a resonating-valence-bond theory*

Pauling (1949) has suggested that in the transitional metals some of the *d* electrons of the inner quantum level are involved in bond formation due to hybridization with the *s* and *p* states of the outer quantum level. He has further shown that provided the amount of *d* character of the bond orbitals is known the single-bond radius for an atom can be calculated and that this value can be corrected for the appropriate bond number when the element occurs in a structure. Assuming that the amounts of *d* character of the manganese atoms in the compound $MnAl_6$ do not vary greatly from those in the metal, it is possible to calculate the average interatomic distances which would be expected in the structure.

The single bond radius for normal manganese is 1·171 Å and for aluminium 1·248 Å. Regarding the manganese valency as +6, the characteristic valency for the transitional metals, the bonds to the ten aluminium ligates will have bond numbers $n = 3/5$ and the correction to the radius is equal to 0·133 Å. The sum of these three numbers, 2·552 Å, gives the predicted value of the Mn–Al distance and is in extremely good agreement with the observed distance of 2·56 Å. The average distance between the aluminium atoms can be calculated in a similar fashion, but the value of 2·898 Å obtained is very much higher than the observed distance of 2·78 Å. In making a more refined calculation for the Co–Al and Al–Al distances in the Co_2Al_9 structure, Pauling (1951) assumes the transfer of one electron from the cobalt atoms to the aluminium atoms, and obtains values for these distances which are in essential agreement with those observed by Douglas (1950).

The arguments upon which these calculations are based directly contradict Raynor's hypothesis. The accuracy of the predicted values for the distances between the transitional metal atoms and the aluminium atoms is striking, but the method provides only indirect evidence of the direction of electron transfer and the results at this stage must be regarded as based upon much empirical evidence. Pauling (1951) has already pointed out that additional experimental evidence capable of distinguishing between the two hypotheses could be provided by a study of the magnetic properties of the compounds.

8. Conclusion

The results discussed in the previous section, with the exception of § 7(iv), support the view that in $MnAl_6$ the manganese atoms do absorb free electrons into their 3*d* orbitals, but to what extent it is difficult to say. The counts support the evidence given by Robinson, from his examination of the Mn_3SiAl_9 structure, that the effect is smaller than is suggested by Raynor. Doubt as to the accuracy of the electron counts is likely to remain until the intensities of the reflexions are directly measured on an absolute scale. The direct determination of the atomic scattering factor parameters for the manganese atom in the element also appears to be a necessary preliminary to the full discussion of the significance of this structure, as the effects sought are so small. The full significance of the shortened bond distances observed in the structure is more likely to be realised when the analysis of similar structures at present under investigation has been completed. It is, however, difficult to avoid the conclusion that they are a direct result of the operation of electronic factors governing the formation and stability of the structure.

I am indebted to Prof. Sir Lawrence Bragg and to Dr W. H. Taylor for the provision of facilities and many helpful discussions during the progress of the work in Cambridge. In Sheffield I have been indebted to Mr D. A. Oliver for the provision of facilities which enabled the work to be completed and for his encouragement and interest in its progress. I have to thank the British Iron and Steel Research Association for financial support for the greater part of the time during which this work was being done.

References

Albrecht, R. (1939). *Rev. Sci. Instrum.* **10**, 221.

Axon, H. J. & Hume-Rothery, W. (1948). *Proc. Roy. Soc.* A, **193**, 1.

Booth, A. D. (1946). *Proc. Roy. Soc.* A, **188**, 77.

Cochran, W. (1950). *Acta Cryst.* **3**, 268.

Cochran, W. (1951). *Acta Cryst.* **4**, 81.

Cruickshank, D. W. J. (1949). *Acta Cryst.* **2**, 65.

Douglas, A. M. B. (1950). *Acta Cryst.* **3**, 19.

Farquhar, M. C. M. & Lipson, H. (1946). *Proc. Phys Soc. Lond.* **58**, 200.

Hofmann, U. (1938). *Aluminium, Berl.* **20**, 867.

Howells, E. R., Phillips, D. C. & Rogers, D. (1950). *Acta Cryst.* **3**, 210.

Jones, H. (1934). *Proc. Roy. Soc.* A, **144**, 225.

Köster, W. & Bechthold, W. (1938). *Z. Metallk.* **30**, 294.

Nicol, A. D. I. (1951). Dissertation for Ph.D. degree, Cambridge.

Pauling, L. (1938). *Phys. Rev.* **54**, 899.

PAULING, L. (1949). *Proc. Roy. Soc.* A, **196**, 343.
PAULING, L. (1951). *Acta Cryst.* **4**, 138.
PHILLIPS, H. W. L. (1943). *J. Inst. Met.* **69**, 275.
PRATT, J. N. & RAYNOR, G. V. (1951). *Proc. Roy. Soc.* A, **205**, 103.
RAYNOR, G. V. & HUME-ROTHERY, W. (1943). *J. Inst. Met.* **69**, 415.
RAYNOR, G. V. & WAKEMAN, D. W. (1947). *Proc. Roy. Soc.* A, **190**, 82.
RAYNOR, G. V. & WALDRON, D. M. B. (1948). *Proc. Roy. Soc.* A, **194**, 362.
ROBINSON, K. (1952). *Acta Cryst.* **5**, 397.
VIERVOLL, H. & ÖGRIM, O. (1949). *Acta Cryst.* **2**, 277.
WILSON, A. J. C. (1949). *Acta Cryst.* **2**, 318.

Acta Cryst. (1953). **6**, 293

Détermination des Oscillations d'Agitation Thermique des Atomes Engagés dans un Cristal: Cas de la Structure Type Fluorine

PAR D. CRIBIER*

Laboratoire de Physique Théorique du Collège de France, Paris, France

(*Reçu le* 1 *juillet* 1952)

The frequency and form of thermal vibrations are determined by the Fourier matrix. If the crystalline motif is composed of g atoms, this is a Hermitian matrix of order $(3g \times 3g)$ containing (for an asymmetrical crystal) $3g(3g+1)/2$ elements. Just as the crystal symmetry reduces the number of coefficients of elasticity, so it reduces the number of independent elements of the Fourier matrix and permits the algebraic nature of these elements to be determined.

In this paper the symmetry operations are applied to determine the number of independent elements in the Fourier matrix of the structure of fluorite, CaF_2, and to determine the nature of the atomic oscillations when these oscillations are controlled by vectors parallel to the symmetry axes.

The oscillations controlled by wave vectors parallel to the tetrad or triad axes are transverse degenerate or rectilinear longitudinal. The oscillations of the calcium atoms controlled by a wave vector parallel to the diad axes are rectilinear, longitudinal or transverse. Three of the oscillations of a fluorine atom controlled by a wave vector parallel to the diad axes are rectilinear longitudinal; the six other oscillations are elliptical, the plane of vibration being defined by the diad axis parallel to the wave vector and the perpendicular tetrad axis.

1. Symbolisme et définition

La position d'un atome m, j situé dans le motif cristallin m en position j est définie par la somme des 3 vecteurs:

$$\mathbf{m}+\mathbf{j}+\mathbf{u}_j^m .$$

Si les vecteurs $\mathbf{l}_i$ sont les périodes du milieu cristallin, $(i = 1, 2, 3)$:

$$\mathbf{m} = \sum_i m_i \mathbf{l}_i \; (m_i = \ldots, -2, -1, 0, 1, 2, \ldots) .$$

$\mathbf{m}$ va de l'origine du réseau, (nœud 0, 0, 0) au nœud (m_1, m_2, m_3) contenu dans le motif cristallin m.

$$\mathbf{j} = \sum_i j_i \mathbf{l}_i \quad |\mathbf{j}_i| \leq 1 .$$

$\mathbf{j}$ va du nœud (m_1, m_2, m_3) à la position moyenne de l'atome j dans le motif cristallin.

$\mathbf{u}_j^m$ est le vecteur élongation qui va de la position moyenne de l'atome m, j à sa position instantanée.

Faisant usage d'axes de coordonnées rectangulaires Ox_α, $(\alpha = 1, 2, 3)$, V_α sera la projection orthogonale du vecteur $\mathbf{V}$ sur l'axe Ox_α; μ_j est la masse de l'atome j; on notera $\overline{X}$ la grandeur complexe conjuguée de la grandeur X.

Les forces de rappel interatomiques sont déduites de la fonction énergie potentielle du cristal en supposant valable la loi de Hooke pour les déplacements des atomes dus à l'agitation thermique. La force de rappel globale $\mathbf{F}_j^m$ appliquée à l'atome m, j a pour composantes:

$$F^{m}_{\underset{\alpha}{j}} = \sum_{pk\beta} c^{m-p}_{\underset{\alpha\beta}{jk}} . u^{p}_{\underset{\beta}{k}} .$$

Les indices j et k courent de 1 à g, s'il y a g atomes par motif cristallin.

Les indices m et p courent de 1 à n, s'il y a n motifs cristallins dans le cristal.

Les coefficients $c^{m-p}_{\underset{\alpha\beta}{jk}}$ sont les composantes constantes d'un tenseur C^{m-p}_{jk} du 2ème ordre dans l'espace à trois dimensions, covariant et symétrique en α et β:

$$C^{m-p}_{jk} = C^{p-m}_{kj} .$$

Les tenseurs $C^{0}_{\underset{\alpha\beta}{jj}}$ sont tels que:

---

* Stagiaire de recherches au C.N.R.S.